Received: 12 September 2020 | Accepted: 16 February 2021

DOI: 10.1002/sctm.20-0424

TISSUE-SPECIFIC PROGENITOR AND STEM CELLS

STEM CELLS TRANSLATIONAL MEDICINE

Type II collagen-positive embryonic progenitors are the major contributors to spine and intervertebral disc development and repair

Xinhua Li[1,2,3] | Shuting Yang[1] | Ling Qin[4] | Shuying Yang[1,5,6]

[1]Department of Basic and Translational Sciences, School of Dental Medicine, University of Pennsylvania, Philadelphia, Pennsylvania, USA

[2]Department of Orthopedics, Shanghai General Hospital, Shanghai Jiao Tong University School of Medicine, Shanghai, People's Republic of China

[3]Department of Spinal Surgery, East Hospital, Tongji University, School of Medicine, Shanghai, People's Republic of China

[4]Department of Orthopedic Surgery, Perelman School of Medicine, University of Pennsylvania, Philadelphia, Pennsylvania, USA

[5]The Penn Center for Musculoskeletal Disorders, School of Medicine, University of Pennsylvania, Philadelphia, Pennsylvania, USA

[6]Center for Innovation & Precision Dentistry, School of Dental Medicine, School of Engineering and Applied Sciences, University of Pennsylvania, Philadelphia, Pennsylvania, USA

Correspondence
Shuying Yang, PhD, MD, Department of Basic and Translational Sciences, School of Dental Medicine, University of Pennsylvania, 240 South 40th Street, Levy 437, Philadelphia, PA 19104-6030, USA.
Email: shuyingy@upenn.edu

Funding information
China Scholarship Council (CSC), Grant/Award Number: 201706260178; National Institutes of Health, Grant/Award Numbers: AG048388, AR066101, DE023105; National Institute on Aging; National Institute of Arthritis and Musculoskeletal and Skin Diseases; National Institute of Dental and Craniofacial Research

Abstract

Basic mechanism of spine development is poorly understood. Type II collagen positive (Col2+) cells have been reported to encompass early mesenchymal progenitors that continue to become chondrocytes, osteoblasts, stromal cells, and adipocytes in long bone. However, the function of Col2+ cells in spine and intervertebral disc (IVD) development is largely unknown. To further elucidate the function of Col2+ progenitors in spine, we generated the mice with ablation of Col2+ cells either at embryonic or at postnatal stage. Embryonic ablation of Col2+ progenitors caused the mouse die at newborn with the absence of all spine and IVD. Moreover, postnatal deletion Col2 + cells in spine resulted in a shorter growth plate and endplate cartilage, defected inner annulus fibrosus, a less compact and markedly decreased gel-like matrix in the nucleus pulposus and disorganized cell alignment in each compartment of IVD. Genetic lineage tracing IVD cell populations by using inducible Col2-creERT; tdTomato reporter mice and non-inducible Col2-cre;tdTomato reporter mice revealed that the numbers and differentiation ability of Col2+ progenitors decreased with age. Moreover, immunofluorescence staining showed type II collagen expression changed from extracellular matrix to cytoplasm in nucleus pulposus between 6 month and 1-year-old mice. Finally, fate-mapping studies revealed that Col2+ progenitors are essential for IVD repair in IVD injured model. In summary, embryonic Col2+ cells are the major source of spine development and Col2+ progenitors are the important contributors for IVD repair and regeneration.

KEYWORDS
intervertebral disc, lineage-tracing, nucleus pulposus, stem cell, type II collagen

1 | INTRODUCTION

The spine is a complex with vital structure. Its function includes not only structural support of the body as a whole, but it also serves as a conduit for safe passage of the neural elements while allowing proper interaction with the brain.[1-4] Embryologically, a detailed cascade of events occurs to result in the proper formation of the spine. Alterations in spinal embryologic development can result in one or more congenital spinal abnormalities including hemivertebrae, spina bifida, congenital scoliosis, congenital kyphosis, and so on.[1] Although the general embryologic spine development process has been investigated for many years,[4,5] what cell lineages of Col2+ cells can contribute to spine development remain unclear.

With the development of genetic lineage tracing technology, significant progress has been made in understanding specific cell contributions to skeletal and spine development.[6-12] Tracing for Noto-cre mouse, McCann et al revealed notochordal cells might serve as tissue-specific progenitor cells within the disc and notochordal cells and chondrocyte-like nucleus pulposus cells are derived from the embryonic notochord.[13] By tracing type II collagen positive (Col2+) cells, some studies reported that Col2+ cell is one of the widest cell populations in vivo and it encompasses early mesenchymal progenitors that continue to become chondrocytes, osteoblasts, stromal cells, and adipocytes in long bone.[14-16] However, few studies reported the function and distribution of Col2+ cells in mouse spine.

Most recently, Tong et al[17] first reported Col2+ cells presented in endplate cartilage (EP), growth plate (GP), and inter annual fibrosis (IAF) cells in intervertebral disc (IVD) but not in NP at postnatal day (P28) when tamoxifen (TM)-inducible type II collagen Cre (Col2-creERT) mice are injected with TM at P6. Wei et al[18] further reported that Col2+ cells existed in the NP, entire AF, EP, and GP in the lumbar spine in Col2-cre;tdTomato mice. However, how Col2+ cells contribute to spine development and IVD repair and what the dynamic changes of Col2+ cells during IVD development during aging remain unclear.

In this study, we delete Col2+ cells at embryonic and postnatal stages by crossing diphtheria toxin ($DTA^{fl/fl}$) mice with Col2-cre mice and Col2-creERT mice, respectively, and deeply understand the contribution of Col2+ cells to spine and IVD development and maintenance. We found that embryonic deletion of Col2+ cells caused absence of entire spine, whereas postnatal deletion of Col2+ cells resulted in defective IVD components. Moreover, by performing lineage tracing of IVD cell populations using Col2-creERT; tdTomato reporter mice and Col2-cre;tdTomato reporter mice during aging, we found that the numbers and differentiation ability Col2+ progenitors decreased with age. Col2+ progenitors in injured disc are essential contributors to IVD repair in IVD injury mouse model. Our results thus for the first time reveal that Col2+ progenitors play critical role for spine development, IVD maintenance, and repair.

Significance statement

Some studies have reported that type II collagen positive (Col2+) cells encompass early mesenchymal progenitors that continue to become chondrocytes, osteoblasts, stromal cells, and adipocytes in long bone. However, few studies have reported the function and distribution of Col2+ cells in mouse spine and intervertebral disc disease (IVDD). The present study provides the first evidence that Col2+ progenitors are the major source for spine development and the maintenance of spine pattern and IVD and that Col2+ inter annual fibrosis progenitors are essential contributors to IVD repair in IVD injury mouse model. Thus, our findings provide new insights into the spine or IVD development and new therapeutic strategies for IVDD repair and regeneration.

2 | MATERIALS AND METHODS

2.1 | Mice

All procedures regarding housing, breeding, and collection of animal tissues were performed as per approved protocols by the Institutional Animal Care and Use Committee (IACUC) of the University of Pennsylvania, in accordance with the IACUC's relevant guidelines and regulations. All mice used in this study are C57BL mouse strain. Col2-cre,[19] Col2-creERT,[20] R26-tdTomato,[21] $DTA^{fl/fl}$,[22] and Aggrecan-creERT[23] mice were purchased from Jackson laboratory (Bar Harbor, Maine). Col2-cre;$DTA^{fl/-}$ and Col2-creERT;$DTA^{fl/fl}$ mice were generated by breeding $DTA^{fl/fl}$ mice with Col2-cre or Col2-creERT mice. Col2-creERT;$DTA^{fl/fl}$ mice were intraperitoneally (i.p.) injected with TM at indicated time points to induce the postnatal deletion of Col2+ cells. Col2-cre;tdTomato, Aggrecan-creERT;tdTomato, and Col2-creERT; tdTomato were generated by breeding TM-inducible Col2-creERT, Aggrecan-creERT, and Col2-cre mice with R26-tdTomato reporter mice and tdTomato labeled patterns in vertebral bone and IVD at different time points were analyzed. All mice were housed in a specific pathogen-free condition.

TM (T5648, Sigma, St. Louis, Missouri) solution preparation and administration were performed as previously described.[24] Briefly, TM was first dissolved in 100% ethanol (100 mg/mL) and then diluted with sterile corn oil to a final concentration of 10 mg/mL. The TM-oil mixture was stored at 4°C until use. Mice in both control and experiment groups were i.p. administered with same dose of TM (75 mg TM/kg body weight) at the indicated time points.

To better present our data, we simply the information of mice in each figure of Col2-creERT;tdTomato mice as: harvest time (tamoxifen injected date + the tracing time period). For example, P6 (3 + 3) means: in Col2-creERT;tdTomato mice, the mouse harvesting date is

P6 (tamoxifen injected date is P3 and tracing for 3 days). Since all the Col2+ cells activated starting from embryonic stage in Col2-cre; tdTomato mice, we only include the date for harvesting mice sample. For example, P6 means: in Col2-cre;tdTomato mice, the mouse harvesting date is P6.

2.2 | Histology

Mouse lumbar spine tissues (L3-L5) were dissected under a stereomicroscope to remove soft tissues, and fixed in 4% paraformaldehyde, overnight at 4°C, then decalcified in 10% ethylenediaminetetraacetic acid (EDTA) for 14 days at 4°C. Decalcified samples were cryoprotected in 30% sucrose/PBS solutions and then in 30% sucrose/PBS:OCT (1:1) solutions for overnight at 4°C. Samples were embedded in an OCT compound (4583, Sakura, Zoeterwoude, Netherlands) under a stereomicroscope and transferred on a sheet of dry ice to solidify the compound. Embedded samples were cryosectioned at 6 μm using a cryostat (CM1850, Leica).

2.3 | Goldner's Masson trichrome staining

Longitudinal sections of whole tail were cut at 6 μm using a cryostat followed by Goldner's trichrome staining protocol as previously described.[25] Briefly, the slides were mordanted in Bouin's Fluid solution and stained with Weigert's hematoxylin, ponceau acid fuchsin and then costained with light green respectively. Five to six mice were evaluated in each group.

2.4 | H&E staining and Safranin O/fast green staining

Mice IVD between the fourth and fifth lumbar spine tissues (L4-L5) or Co disc between the fifth and seven Co vertebrae (Co5-7) were sectioned and stained with H&E and Safranin O/fast green staining. Safranin O/fast green staining was performed to visualize cartilage and assess proteoglycan content as described previously.[26,27] The Slides from each sample were stained with Weigert's iron hematoxylin and fast green, and then stained with 0.1% Safranin O solution.

2.5 | Alizarin red/Alcian blue staining

The skeleton from each mouse were stained with Alizarin red/Alcian blue reagents as reported previously.[24] Briefly, mice tail was fixed with 90% ethanol, and then stained with 0.01% Alcian blue solution (26385-01, Electron Microscopy Sciences, Washington, Pennsylvania) and 1% Alizarin red S solution (A47503, Thomas Scientific,Swedesboro, New Jersey), respectively. Stained skeletons were stored in glycerol.

2.6 | Scanning electron microscopy

Caudal spine discs (C7/8) from 4-week-old Col2-creERT or Col2-creERT;DTA$^{fl/fl}$ mice were dissected and fixed in 2.5% (v/v) glutaraldehyde at 4°C. The collagen fiber diameters were measured using SEM analysis as described previously.[28] Briefly, the samples were digested in 20.4 U/mL hyaluronidase (H3506, Sigma, St. Louis, Missouri) and 0.1 mg/mL bovine pancreatic trypsin (T1426, Sigma, St. Louis, Missouri). The fixed samples were washed three times with PBS. The specimens were dehydrated in a graded ethyl alcohol (EtOH) series (30%, 50%, 70%, 80%, 90%, and 100%). Subsequently, specimens were dehydrated in ethanol and hexamethyldisilizane (HMDS) solutions, starting with EtOH: HMDS (1:1) and serially increasing to EtOH: HMDS (1:4), and finally washed with 100% HMDS. The samples were air dried in the fume hood for 1 hour. Samples were mounted on the Al-hold with super glue and coated with carbon. The FEI XL30 ESEM (FEI XL30 ESEM, FESEM, Thermo Fisher Scientific, Hillsboro, Oregon, voltage: 8 kV) was used for imaging. ImageJ software was used for the measurement of collagen fibril diameters.

2.7 | Real-time RT-PCR analysis

Whole IVD tissues were dissected respectively from lumbar and caudal discs of 4-week-old Col2-creERT or Col2-creERT;DTA$^{fl/fl}$ mice, and immediately placed in Trizol for RNA isolation (15596018, Thermo Fisher Scientific, Swedesboro, New Jersey). cDNA was synthesized from 2 μg of total RNA. qPCR was performed with SYBR Green PCR master Mix (B21202, Bimake, Sylvanfield, Houston). All qPCR reactions were run in triplicate and normalized to the expression of GAPDH. Each reaction was run in triplicate and independently repeated three times. The sequences and product lengths for each primer pair were included in Supplementary Table 1.

2.8 | Immunofluorescence microscopy

Coronal disc tissue sections with 6 μm thickness were gently rinsed with PBS and incubated with proteinase K (20 μg/mL, D3001-2-5, Zymo Research) for 10 minutes at room temperature (RT). Subsequently, sections were blocked in 5% normal serum (10000 C, Thermo Fisher Scientific, Swedesboro, New Jersey) in PBS-T (0.4% Triton X-100 in PBS) or incubated with antibodies against type II collagen (1:100, ab34712, Abcam) in blocking buffer at 4°C for overnight, and then incubated in second antibodies Alexa Fluor 488-conjugated anti-rabbit (1:200, A11008, Invitrogen, Carlsbad, California) or

Alexa Fluor 647-conjugated anti-mouse (1:200, A-21236, Invitrogen, Carlsbad, California) antibodies for 1 hour at RT. Coverslips were mounted with Fluoroshield (F6057, Sigma-Aldrich, St. Louis, Missouri).

To quantify the percentage of tdTomato+ cells, multiple fields of Z-stacked pictures were randomly captured. At least 30 images were measured. The percentage of tdTomato+ cell was calculated from the ratio of tdTomato+ cells over total cells observed in each compartment of each sample (five sections per sample). Six mice were evaluated in each group. Assessments were independently completed by two investigators who were blinded to the treatment or groups. The average percentage of tdTomato+ cells in each sample and group were pooled and calculated by two investigators.

2.9 | Cell culture

Cells in in juried disc were isolated following the previous report[26,29] with slight modification. Briefly, disc tissues digested initially with protease (53702-25KU, EMD Millipore, Boston, Massachusetts) for 1 hour with agitation on a shaker, followed by collagenase-P (11213865001, Sigma-Aldrich, St. Louis, Missouri) for another 12 hours at 37°C. The digested cells were then transferred for flow cytometry sorting and cell culture at 37°C in a humidified atmosphere with 5% O_2 and 10% CO_2 for 7 to 10 days.

2.10 | CFU-F assay and in vitro differentiation potential test

These protocols were modified from a previous report.[29,30] For CFU-F assays, sorted IAF cells were directly plated in six-well plates at a density 10 cells/cm^2. The cells were incubated at 37° in a humidified atmosphere with 5% O_2 and 10% CO_2 for 7 to 10 days. CFU-F colonies were counted after 7 to 10 days of culture.

For in vitro differentiation assay, tdTomato+ cells were sorted and plated into each well of 48-well plates and cultured for 14 days. Adipocyte, chondrocyte, and osteoblastic differentiation were induced with different differentiation media and then stained with Oil red O (O0625-25G, Sigma-Aldrich, St. Louis, Missouri), Alcian blue (26385-01, Electron Microscopy Sciences, Washington, Pennsylvania) and Alizarin red (A47503, Thomas Scientific, Swedesboro, New Jersey), respectively.

2.11 | Tail injury surgery

The tail injury surgery was performed in 4-week-old Col2-creERT; tdTomato mice when TM injected at P21 as described previously.[26] Briefly, under anesthesia, the mouse coccygeal (Co) IVDs were injured by inserting a 28-G needle into IVD space until the needle tip reached 2/3 of the disc thickness under fluoroscopic guidance with a Faxitron MX-20 (Faxitron X-Ray). Co5/6 in each mouse was injured, whereas mouse Co6/7 without injury was served as intact controls.

2.12 | Statistics

All data are presented as mean ± SD. Shapiro-Wilk test for the normality and Bartlett test for variance were performed to determine the appropriate statistical tests. Student's test for the comparison between two groups or one-way ANOVA followed by Tukey's multiple comparison test for multiple groups was performed. The number of animals and repetitions of experiments were presented in figure legends. The program GraphPad Prism software (GraphPad Software, Inc, San Diego) was used for these analyses. $^*P < .05$, $^{**}P < .01$, $^{***}P < .0001$. NS, not statistically significant.

3 | RESULTS

3.1 | Ablation of embryonic Col2+ progenitors in mice causes absence of the spine

To ablate Col2+ progenitors from mice embryonic stage (Col2-cre; DTA$^{fl/-}$;mutant group), the mice bearing a DTA transgene downstream of a floxed stop condon (DTA$^{fl/fl}$) were bred with Col2-cre transgenic mice. Col2-cre littermates serve as control (wild type). Col2-cre;DTA$^{fl/-}$ mice die at newborn or a few hours after birth. The gross appearance showed severe developmental defects in newborn mice including severe dwarfish with extremely short four limbs and tail (Figure 1A). Skeletal radiographs examination of the control newborns revealed vertebrate were well calcified, while it is completely absence in Col2-cre; DTA$^{fl/-}$ mice (Figure 1B). Furthermore, Alizarin red/Alcian blue staining of mutant newborn showed no positive signaling in spine (Figure 1C), confirming the ablation of Col2+ cells caused absence of the spine.

To gain further insights into the function of Col2+ cells in vertebral development, we did Goldner's Masson trichrome staining in tail of wild type and mutant newborns through sagittal section. In wild type newborns, all the vertebral bone, IVD and skin were well stained and vertebral bone were clearly identified. However, there are not any vertebral bones or IVD in mutant mice (Figure 1D). Higher magnification pictures showed the skin and some muscle or connective tissues in mutant mice were well maintained and the space for vertebral bone were filled with some connective tissues (Figure 1E). Most interestingly, the skin is much thicker in mutant newborn comparing with control (290 μm in wild type mice vs 600 μm in mutant mice) (Figure 1F).

3.2 | Postnatal deletion of Col2+ cells disrupt the spine pattern

To assess the contribution of the postnatal Col2+ cells to vertebrate bone and IVD development, we genetically ablated those cells by generating Col2-creERT;DTA$^{fl/fl}$ via breeding DTA$^{fl/fl}$ with TM inducible Col2-creERT mice and applied with TM at P3 of age. The mice were then harvested at 4-week-old. Skeletal radiographs and Alizarin red and Alcian blue staining showed that Col2-creERT;DTA$^{fl/fl}$ mice have shorter vertebral and tail length (Figure 2A-C). Quantitative analysis

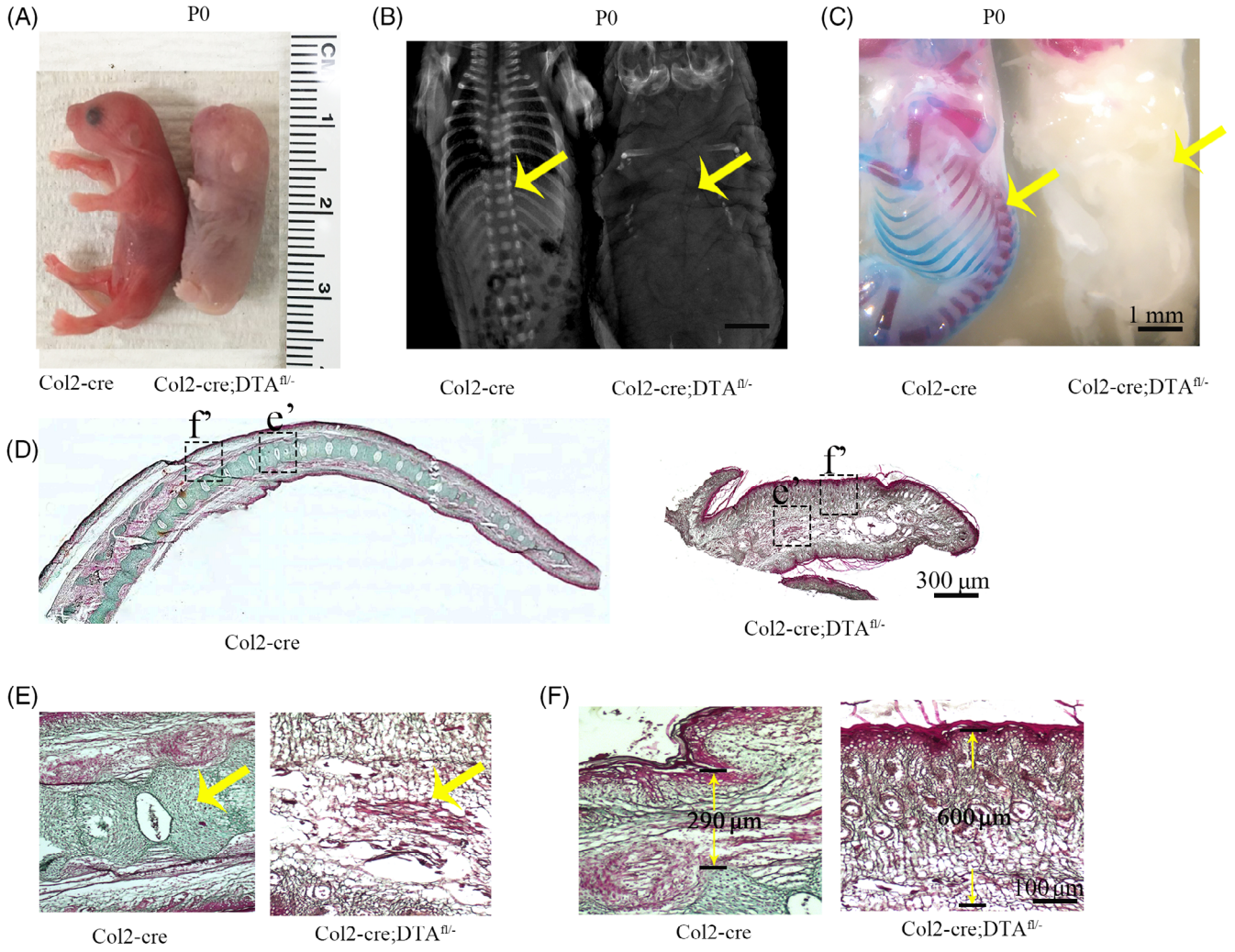

FIGURE 1 Ablation of embryonic Col2+ progenitors in mice causes absence of the spine. A, Gross appearance of Col2-cre, and Col2-cre;DTA$^{fl/-}$ mice at P0. B, X-ray images for P0 Col2-cre, and Col2-cre;DTA$^{fl/-}$ mice. Yellow arrow: spine is completely absent in mutant newborn compared to Col2-cre control. C, Alizarin red and Alcian blue staining of newborn Col2-cre and Col2-cre;DTA$^{fl/-}$ mouse. Yellow arrow: spine complete loss in mutant newborn. Scale bar = 1 mm. D, The tail of Col2-cre and Col2-cre;DTA$^{fl/-}$ newborns mice stained by Goldner's trichrome. Scale bar = 300 μm. E,F, Higher magnification of Golden staining in tail vertebra and skin. Yellow arrow: vertebral and intervertebral disc (IVD) complete loss in mutant newborn. Six mice evaluated in each group. Scale bar = 100 μm

showed the length of third to fifth lumbar vertebral (L3-L5) in Col2-creERT;DTA$^{fl/fl}$ mice much shorter (4.5 mm) compared to that in wild type (7.48 mm) (Figure 2B). Additionally, Col2-creERT;DTA$^{fl/fl}$ mice clearly showed spine epiphyseal dysplasia and flattened vertebral bodies compared to the control.

Safranin O/fast green staining of spine section (L4-L5) from 4-week-old Col2-creERT and Col2-creERT;DTA$^{fl/fl}$ mice showed that the pattern of vertebrae and IVD were shorter and dramatically disrupted in postanal Col2+ cell ablation mice (Figure 2D). Higher magnification examination of the IVD showed that the stereotypical columnar structure of the chondrocytes in the GP was disrupted and that the height of GP and EP region was apparently reduced in mutant mice (Figure 2E,F). Moreover, the AF cells were hypertrophic and NP cells and surrounding gel-like matrixes were dramatically lost in contrast to the wild type (Figure 2G,H).

By analyzing Col2α1 expression and extra cellular matrix (ECM) change in IVD by immunofluorescence staining, we found that Col2α1 expression was dramatically reduced in every compartment of IVD including GP, EP, AF cells and matrix surrounding the NP compared to those in wild type mice (Figure 2I-L). Most noticeably, Col2α1 matrix surrounding the NP was completely lost in Col2+ cell ablated mice (Figure 2I,J). F-actin staining result showed that the cell alignment and interaction in NP and AF are dramatically disrupted indicating Col2+ cells are essential for driving tissues pattern organization (Figure 2M,N).

3.3 | Postnatal deletion of Col2+ cells impair IVD extracellular matrix formation and organization

To further examine whether ablation of Col2+ cells at postnatal stages alters fibrous structure formation and organization in the IVD, we

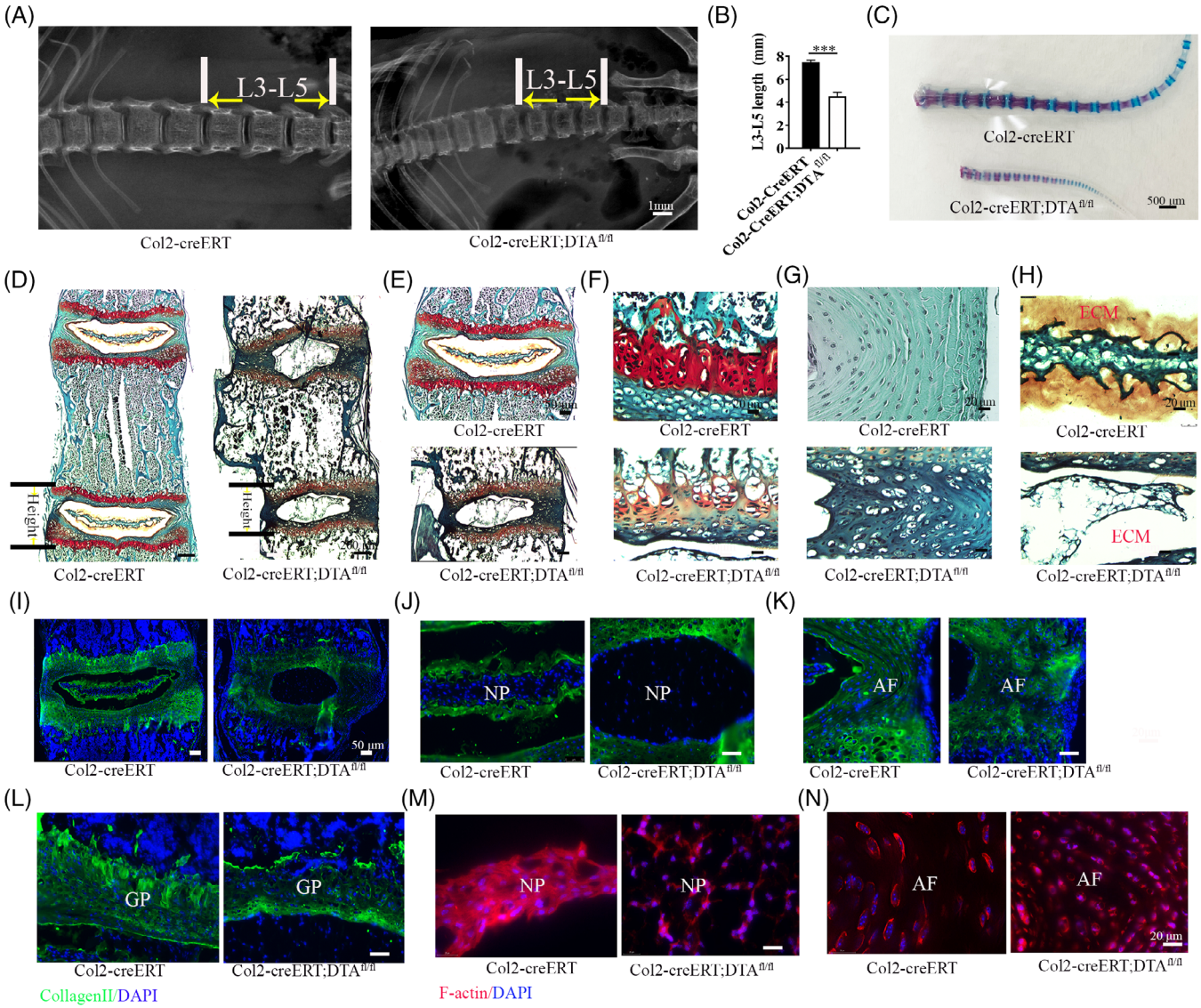

FIGURE 2 Postnatal deletion of Col2+ cells disrupt the pattern of spine. A, X-ray of spine in 4-week-old Col2-creERT and Col2-creERT;DTA$^{fl/fl}$ mice. Scale bar = 1 mm. B, The quantity analysis of mice L3-L5 length of (A) (n = 6 mice per condition from three independent experiments). Data are mean ± SD. C, Alizarin red and Alcian blue staining for the tail from the 4-week-old Col2-creERT and Col2-creERT;DTA$^{fl/fl}$ mice. Scale bar = 500 μm. D, Safranin O/fast green staining of coronal sections of L4-5 spine in 4-week-old Col2-creERT and Col2-creERT;DTA$^{fl/fl}$ mice. Scale bar = 200 μm. E-H, High magnification pictures showing growth plate (GP), AF, and NP in 4-week-old Col2-creERT and Col2-creERT;DTA$^{fl/fl}$ mice. Scale bar = 20 μm. I, Immunofluorescence staining for Col2α1 in intervertebral disc (IVD) of 4-week-old Col2-creERT and Col2-creERT;DTA$^{fl/fl}$ mice. Scale bar = 50 μm. J-L, High magnification immunofluorescence pictures showing Col2α1 protein expression in NP, AF, and GP from 4-week-old Col2-creERT and Col2-creERT;DTA$^{fl/fl}$ mice. M,N, Phalloidin staining show the cytoskeleton of NP and AF in 4-week-old Col2-creERT and Col2-creERT;DTA$^{fl/fl}$ mice. Statistical significance was determined by one-way ANOVA and Student's *t* test. **P* < .05, ***P* < .01, ****P* < .0001. NS, not statistically significant. Scale bar = 20 μm

dissected the Co7-8 and employed scanning electronic microscope (SEM) to observe the ECM in NP and AF of Col2-creERT;DTA$^{fl/fl}$ with TM injection at P3 and harvesting P30. We found that the NP in Col2-creERT;DTA$^{fl/fl}$ is smaller than the control (Supplementary Figure 1A,B). SEM images showed the collagen fiber in control AF and NP well organized in a regular pattern and with similar collagen diameter (Supplementary Figure 1C). In contrast, the collagen arrangement in AF and NP were markedly distorted and disorganized and collagen diameter are varied and thinner in Col2-creERT;DTA$^{fl/fl}$ mice (Supplementary Figure 1C). Quantitative analysis revealed that the average diameter of collagen fibrils was significantly decreased from 75.3 μm in control Col2-creERT mice to 37.2 μm in Col2-creERT;DTA$^{fl/fl}$ mice, indicating that postnatal Col2+ cells plays an essential role for the proper arrangement of collagen fiber in IVD (Supplementary Figure 1D).

To investigate how ablation of Col2+ cells affects ECM related genes' expression in IVD, mouse IVDs were isolated from Col2-creERT and Col2-creERT;DTA$^{fl/fl}$ mice which were injected with

TM at P3 and harvested at P30, and then the total RNA was extracted from these samples. Real time RT-qPCR results showed that the expression level of Col2α1 was significantly decreased in Col2-creERT;DTA$^{fl/fl}$ group, confirming efficient cell ablation (Supplementary Figure 1E). The levels of Col2α1, Aggrecan, Sox9, Col1α1, and Col1α2 in Col2+ cells ablation IVDs were significantly decreased comparing with the control IVDs, indicating that Col2+ cells are important for the IVD ECM gene expression and maintenance. In addition, no significantly change in gene expression levels of matrix metalloproteinase3 (MMP3), matrix metalloproteinase13 (MMP13), A disintegrin and metalloproteinase with thrombospondin motifs-4 (ADAMTS4), a classical marker of degeneration,[31] in IVDs between Col2-creERT and Col2-creERT;DTA$^{fl/fl}$ mice, indicating the ECM decrease are caused by the Col2+ cells ablation not by ECM degradation (Supplementary Figure 1E).

3.4 | Spatial distribution of Col2+ cells in the mouse IVD and vertebral bone

To investigate the contribution of Col2+ cells to IVD development at embryonic and postnatal stages, we traced the fate of Col2-expressing cells in Col2-cre;tdTomato mice and TM inducible Col2-creERT;tdTomato mice by i.p. administering TM at different ages and harvesting them at the indicated time points.

To examine how Col2+ cells contribution to IVD development starting from embryonic stage, we analyzed Col2-cre;tdTomato mice and found that at P0, Col2+ cells can be detected in most cells in IVD or vertebral bone. However, tdTomato fluorescence intensity was weak in NP, GP, EP, and IAF and strong in OAF and vertebral bone. Interestingly, tdTomato+ cells became prominent in every compartment of IVD at P6 and weaker in OAF and vertebral bone compared

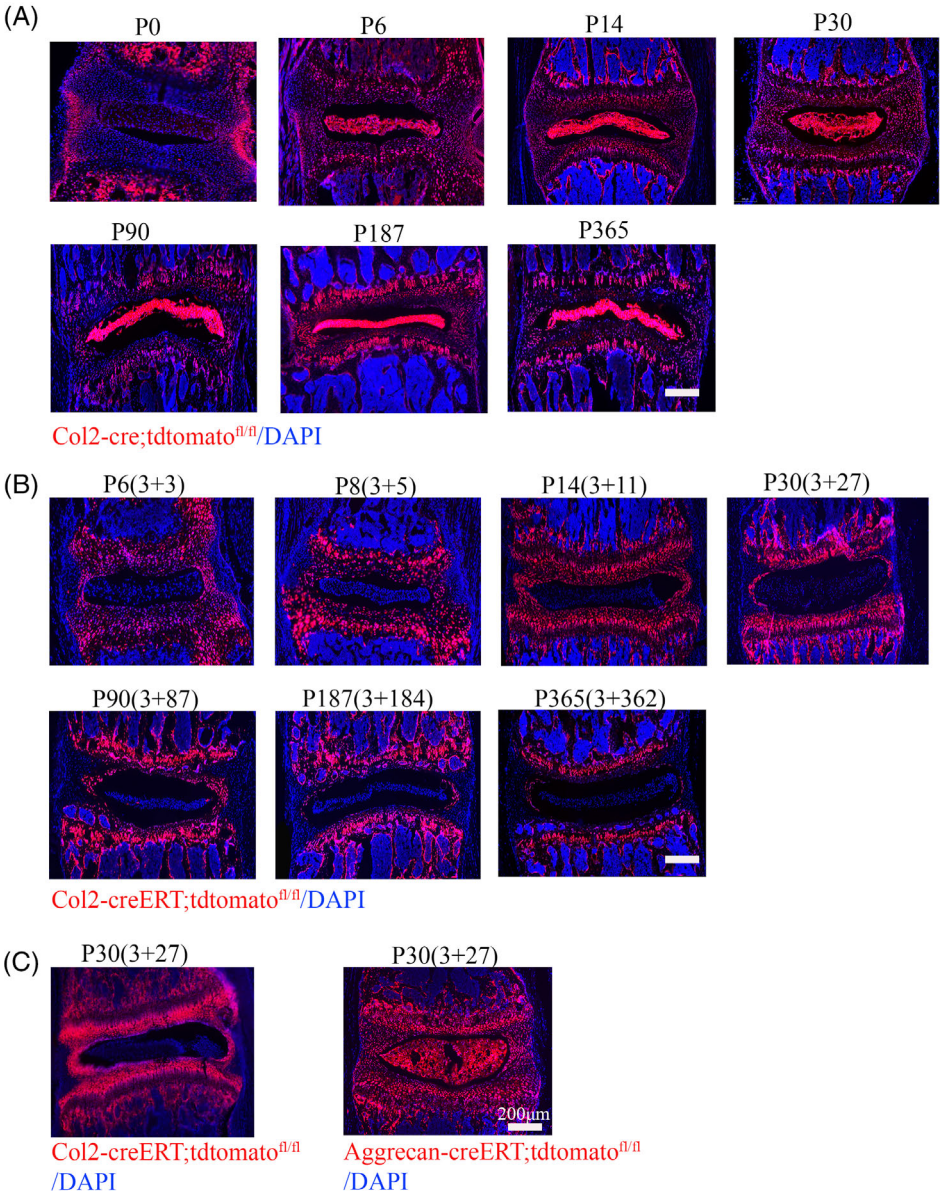

FIGURE 3 Spatial distribution of embryonic and postnatal Col2+ cells in the mouse intervertebral disc (IVD) and vertebral bone. A, Representative images from lineage tracing of embryonic Col2+ cells in IVD at different time point (P0, P6, P14, P30, P90, P187, and P365) in Col2-cre; tdTomato mice. Six mice evaluated in each group. B, Representative images from lineage tracing of Col2 + cells in IVD at different time point (P6, P8, P14, P30, P90, P187, and P365) in Col2-creERT;tdTomato mice. Tamoxifen (75 mg TM/kg body weight) were i.p. injected into P3 mice. Six mice evaluated in each group. C, Representative images from lineage tracing tdTomato+ cells in IVD from Col2-creERT;tdTomato and Aggrecan-creERT;tdTomato mice at P30. Tamoxifen (75 mg TM/kg body weight) were i.p. injected into P3 mice. Six mice evaluated in each group. Scale bar = 200 μm

to P0. After P6 and thereafter, strong fluorescence tdTomato+ cells gradually increase in each compartment of IVD and in vertebrae cortical or trabecular bone (Figures 3A and 4A). Quantity analysis showed the 90.7%, 92.2%, 94%, 94%, and 94.8% of tdTomato+ cells in trabecular bone at P0, P6, P14, P30, and P90, respectively, in Col2-cre; tdTomato mice (Figure 4B). About 91%, 92.3%, 93%, 94%, and 94.3% of tdTomato+ cells in cortical bone at P0, P6, P14, P30, and P90, respectively, in Col2-cre;tdTomato mice.

To further examine how Col2+ cells contribute to spine development from the postnatal stage, Col2-creERT;tdTomato mice were i.p. administered with TM at P3 and harvested at P6, P14, P30 and P90 (Figures 3B and 4C). (To better present our data, we simplified the time information in each figure as: harvest time (TM injected date + the tracing time period.) For example, P6 (3 + 3) means: in Col2-creERT;tdTomato mice, the date for harvest is P6 (TM injected date is P3 and tracing for 3 days). At P6, Col2+ cells were found predominantly in the GP, IAF, EP, the vertebral bone, and osteocytes embedded in bone matrix, and only few tdTomato+ cells can be detected in NP. Interestingly, we noticed the percentage of tdTomato+ cells gradually increased in vertebral bone with age. Quantitative analysis showed that 9.1% of cells were tdTomato+ in trabecular bone at P6, which increased to 14.8%, 17.3%, and 29.8% at P14, P30, and P90, respectively (Figure 4D), and about 4% of cells were tdTomato+ in cortical bone at P6, which increased to 5.5%, 7%, and 7.7% at P14, P30, and P90, respectively, in Col2-creERT;tdTomato mice with TM injection at P3. These results suggested that osteoblasts or osteocytes differentiate from Col2+ cells.

To exclude the possibility that few Col2+ cells in NP is caused by the fact that TM cannot efficiently enter into NP to induce tdTomato expression in NP of Col2-creERT;tdTomato mice, we i.p. injected same dose of TM to Aggrecan-CreERT;tdTomato transgenic mice to induce Cre-recombination. Figure 3C showed almost all NP cells are aggrecan+ confirming that TM can enter and induce cre expression in NP. The fact of different expression pattern between Col2-creERT; tdTomato and Aggrecan-creERT;tdTomato indicated NP can express aggrecan but not Col2α1 at P3.[23]

3.5 | The decreased numbers and differentiation ability of Col2+ progenitors during aging

To explore how age affect Col2+ progenitors fate at IVD, Col2-creERT;tdTomato mice were injected TM at age of P3, P21, P27, P87, P184, P362, and the mice were harvested at 3 days later follow each

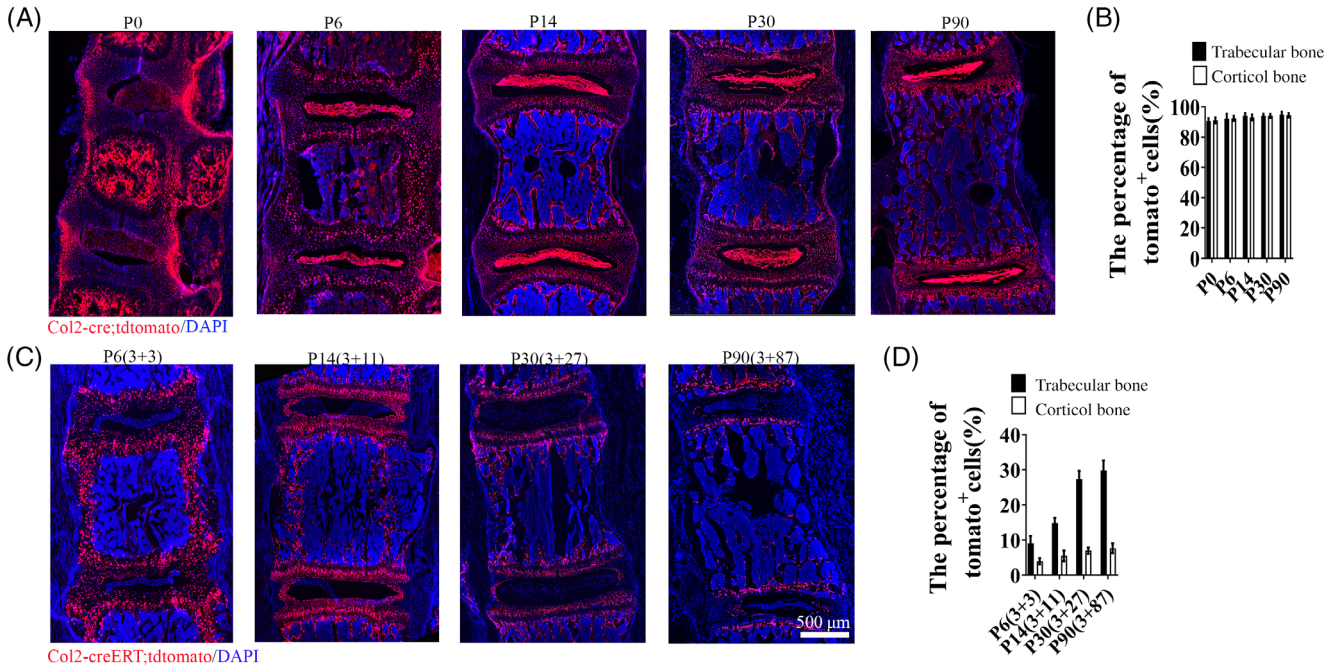

FIGURE 4 Lineage tracing Col2+ cells in spine and intervertebral disc (IVD) at different time points. A, Lineage tracing Col2+ cells in spine and IVD at P0, P6, P14, P30, and P90 in Col2-cre;tdTomato mice. (Since all the Col2+ cells activated from embryonic stage Col2-cre;tdTomato mice, we only include the date for harvesting mice sample in each group. For example, P6 means: in Col2-cre;tdTomato mice, the date for harvest is P6.) B, Quantitative measurements of the percentage of tdTomato+ cells to the total DAPI+ cells in (A) (n = 6 mice per condition from three independent experiments). Data are mean ± SD. C, Lineage tracing Col2+ cells in spine and IVD at P6, P14, P30, and P90 in Col2-creERT; tdTomato mice. Tamoxifen (75 mg TM/kg body weight) were i.p. injected into P3 mice. Six mice evaluated in each group. (The data presented: harvest time (tamoxifen injected date + the tracing time.) For example, P6 (3 + 3) means: in Col2-creERT;tdTomato mice, the date for harvest is P6 (TM injected date is P3 and tracing for 3 days). D, Quantitative measurements of the percentage of tdTomato+ cells to the total DAPI+ cells in (C) (n = 6 mice per condition from three independent experiments). Data are mean ± SD. Statistical significance determined by one-way ANOVA and Student's *t* test. **P* < .05, ***P* < .01, ****P* < .0001. NS, not statistically significant. Scale bar = 500 μm

injection for analysis of histological sections. As showed in Figure 5A, D, 97.4% of DAPI+ GP chondrocyte were tdTomato+ when TM inject at P3 which were decreased to 94.1%, 50.2%, 39.8%, 18.8%, and 5.1% when TM injected at P21, P27, P87, P184, and P362, respectively. In IAF, 65.4% of DAPI+ cells were tdTomato+ when TM injected at P3, which decreased to 55.4%, 7.9%, 3.1%, 1.3%, and 1.0% when TX injected at P21, P27, P87, P184, and P362. Consistently, 94.5% of DAPI+ EP chondrocytes were tdTomato+ when TM injected at P3, which decreased to 5.6% when TM injected at P21, to 2.7% at P27, to 2.2% at P87, 1.9% at P184, and to 1.5% at P362. For NP cells, 1% of cells were tdTomato+ when TM injected at P3 which were decreased to 0.76% when TM injected at P21, to 0.93% at P27, to 0.9% at P87, 0.58% at P184, and to 0.4% at P362. All these results suggested the Col2+ progenitors significantly decreased during aging process.

To determine how age affects the number and differentiation ability of Col2+ cells, we compared the number of tdTomato+ cells in the IVD at P90 when the tdTomato expression was activated starting from embryonic stage in Col2-cre;tdTomato mice or starting from P3, P30, P60, and P87 with TM injection in Col2-creERT;tdTomato mice.

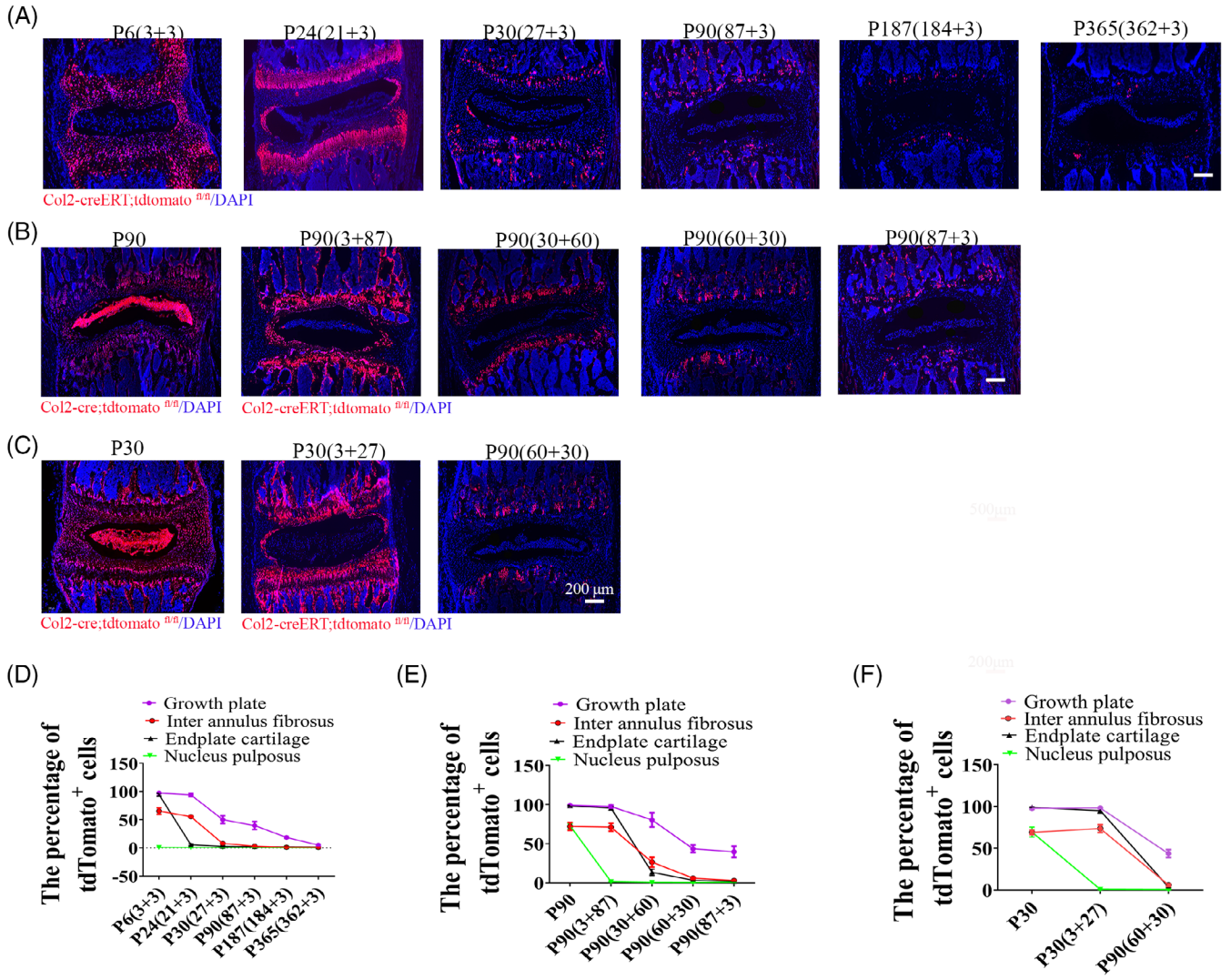

FIGURE 5 The decreased numbers and differentiation ability of Col2+ progenitors during aging. A, Lineage tracing of postnatal Col2+ cells for 3 days in each component of intervertebral disc (IVD) which activated at different time points (P3, P21, P27, P87, P184, and P362). 75 mg/kg tamoxifen were i.p. injected into mice at above indicated different time points. The mice were harvested at day 3 following TM injection. B, Lineage tracing of Col2+ cells in IVD at P90, which was activated at different time points (since embryo, P3, P30, P60, and P87). C, Lineage tracing Col2+ cells in IVD for 1 month while activated at different time point (since embryo, P3, P60). 75 mg/kg tamoxifen were i.p. injected into mice at above indicated different points. D, Quantitative measurements of the percentage of tdTomato+ cells to the total DAPI+ cells in (A) (n = 6 mice per condition from three independent experiments). Data are mean ± SD. E, Quantitative measurements of the percentage of tdTomato+ cells to the total DAPI+ cells in (B) (n = 6 mice per condition from three independent experiments). Data are mean ± SD. F, Quantitative measurements of the percentage of the cells with tdTomato+ to the total DAPI+ cells per view of (C) (n = 6 mice per condition from three independent experiments). Data are mean ± SD. The percentage calculation in each tissue were measured at least 1000 cells each sample. Statistical significance was determined by one-way ANOVA and Student's *t* test. **P* < .05, ***P* < .01, ****P* < .0001. NS, not statistically significant. Scale bar = 200 μm

Quantitative analysis showed the number of tdTomato+ cells gradually decreased in when Col2+ cells activated since embryo (Col2-cre; tdTomato), and at P3, P30, P60, to P87 (Figure 5B,E). Specifically, 99.2% DAPI+ GP chondrocytes were tdTomato+ cells in Col2-cre; tdTomato mice tracing up to P90, while tdTomato+ cells decreased to 97.5%, 80.4%, 43.6%, and 39.8% in Col2-creERT;tdTomato mice when TM was injected at P3, P30, P60, and P87 and cells were traced up to P90, respectively. Similarly, In IAF, tdTomato+ cells in Col2-cre; tdTomato were approximately 72.2% at P90, which decreased to 71.2%, 26.4%, 6%, and 3.1% in Col2-creERT;tdTomato mice when TM injected at P3, P30, P60, and P87. For EP chondrocytes, 98.5% of cells were tdTomato+ in Col2-cre;tdTomato, which decreased to 95.5% in Col2-creERT;tdTomato mice when TM injected at P3, to 13.4% at P30, to 3.4% at P60, and to 2.2% at P87. For NP cells, 73% of cells were tdTomato+ when the Col2-tdTomato+ cell starting from embryonic stage in Col2-cre;tdTomato mice, which decreased to 1.5%, 0.6%, 0.6%, and 0.9% in Col2-creERT;tdTomato mice when TM injected at P3, P30, P60, and P87. All these results suggest the numbers and differentiation ability of Col2+ cells decrease during aging process.

To further confirm the differentiation ability of Col2+ progenitors decreased with age, we compared the tdTomato+ cells in the IVD during 1 month of tracing when tdTomato+ cells were activated starting from embryonic stage in Col2-cre;tdTomato mice, or at P3 (when TM injected at P3 in Col2-creERT;tdTomato mice) and P60 (when TM injected at P60 in Col2-creERT;tdTomato mice) (Figure 5C,F). Approximately 97.7% of DAPI+ GP chondrocytes were tdTomato+ when tdTomato+ cells were activated starting from embryonic stage in Col2-cre;tdTomato mice; however, tdTomato+ cells decreased to 98.2% when TM injected at P3, to 43.6% at P60. In IAF, 69.1% of cells were tdTomato+ cells in Col2-cre;tdTomato mice, which decreased to 73.5% and 6% when TM injected at P3 and P60 in Col2-creERT; tdTomato mice, respectively. For the EP chondrocytes, 98.9% of cells were tdTomato+ in Col2-cre;tdTomato, and those cells decreased to 95.1% when TM injected at P3, to 3.4% at P60 in Col2-creERT; tdTomato mice. For NP cells, 69.3% of cells were tdTomato+ in Col2-cre;tdTomato mice, which decreased to 0.8% and 0.6% when TM injected at P3 and P60 in Col2-creERT;tdTomato mice, respectively. All these data further demonstrated that the differentiation ability of Col2+ progenitors decreased during aging process.

3.6 | The inconsistence of Col2+ cells and type II collagen expression in mice IVD

To better understand the relationship between embryonic or postnatal Col2+ cells and Col2α1 expression, we compared their localization and distribution in IVD at different time points (Figure 6A-D). Specifically, for testing postnatal Col2+ cells, Col2-creERT;tdTomato mice were applied with TM at P5, P27, P184, and P362, respectively, and harvested 3 days later following TM administration. At P6, immunofluorescence staining result showed that Col2α1 expressed in GP, EP, and IAF of IVD, similar to the pattern of Col2+ cells when activated at P3. Consistent with the trend demonstrated previously, the tdTomato + cells in IVD were dramatically decreased from P3 to P362 in Col2-creERT;tdTomato mice. However, Col2α1 protein expression was relatively stable during the process. Interestingly, Col2α1 expression was detected at the gel-like matrix mainly at surrounding regions of the NP without any expression inside NP cells at P30 and P187, however the whole NP becomes Col2α1 expression positive at P365 (Figure 6D). These results indicate that the expression change of Col2α1 in NP from P187 to P365 in mice. The pattern of Col2+ cells in Col2-cre;tdTomato mice were very stable and similar with it described previously from P6 to P365.

3.7 | Col2+ progenitors are important for IVD repair in injured disc

To further investigate the effect of Col2+ cells on IVD repair and regeneration, we created a IVD injured mouse model at Co5-6 and

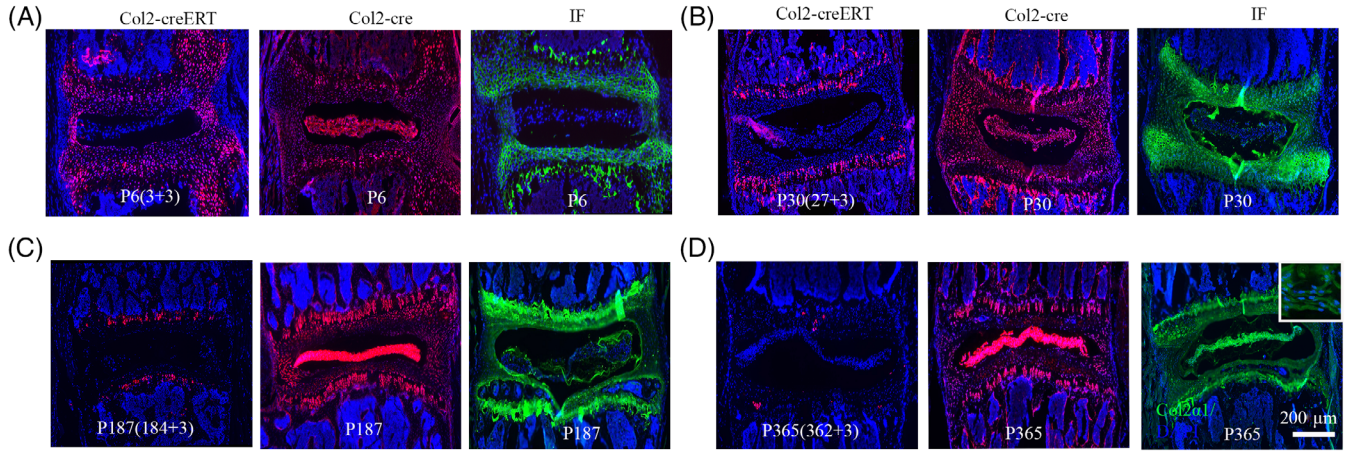

FIGURE 6 The inconsistence of Col2+ cells and type II collagen expression in mice intervertebral disc (IVD). A-D, The expression Col2+ cells by lineage tracing of Col2-creERT;tdTomato, Col2-cre;tdTomato mice, and Col2α1 expression examined by IF staining in IVD at P6 (A), P30 (B), P187 (C), and P365 (D). Six mice were evaluated in each group. Scale bar = 200 μm

compared IVD repair after 2-weeks of healing in Col2-creERT; tdTomato and Col2-creERT;DTA$^{fl/fl}$;tdTomato mice (TM injected at P21) (Figure 7A). As showed in Figure 7B, a much narrowed IVD and severed IVDD can be observed in Col2-creERT;DTA$^{fl/fl}$;tdTomato comparing with Col2-creERT;tdTomato mice indicating Col2+ cells play an important role during IVD repair and regeneration (Figure 7B). To trace the development of IVDD, we measured the disc height index (DHI) in Col2-creERT and Col2-creERT;DTA$^{fl/fl}$ mice following IVD injury and in Col2-creERT intact control. Radiography results showed that DHI gradually decreased from the first week following injury induced IVDD in Col2-creERT and Col2-creERT;DTA$^{fl/fl}$ mice comparing with intact control (Figure 7C,D). Quantitative analysis showed the mean DHI in the Col2-creERT group was 100% in the before of the injury and then became 88.7% ± 3.5%, 85.3% ± 3.4%, and 76.8% ± 4.5% at weeks 1, 2, and 4 following the injury, respectively. In contrast, the DHI decreased to 73.5% ± 7.4%, 36% ± 5.4%, and 3.3% ± 3.9% at weeks 1, 2, and 4 in the Col2-creERT;DTA$^{fl/fl}$ group, respectively (Figure 7D).

To further trace Col2+ cells contribution to IVD repair, we detected the tdTomato+ cells in Col2-creERT;tdTomato and Col2-creERT;DTA$^{fl/fl}$;tdTomato mice with IVD injury as well as Col2-creERT;tdTomato intact control (Figure 7E). In the injured Col2-creERT;tdTomato mice, the IVD exhibited prominent tdTomato+ cells in the GP and IAF space, but few tdTomato+ cells can be detected in injured IVD of Col2-creERT;DTA$^{fl/fl}$;tdTomato mice. Furthermore, H&E staining analysis of mouse IVD at week 4 following IVD injury showed much severer injury in Col2-creERT;DTA$^{fl/fl}$;tdTomato mice compared to Col2-creERT;tdTomato mice (Figure 7F).

To further test the feature of Col2+ progenitors in injured disc, we examined the differentiation ability and CFU-F activity assays. Col2+ progenitors in injured disc were sorted by flow cytometry from 4-week-old Col2-creERT;tdTomato mice. The results showed that around 88.5% of Col2+ cells sorted from injured disc can form CFU-F colonies in vitro (Figure 7G). To assess whether Col2+ progenitors in injured disc behave as stem cells in cell culture, the sorted Col2+ progenitors from injured disc were induced with osteogenic,

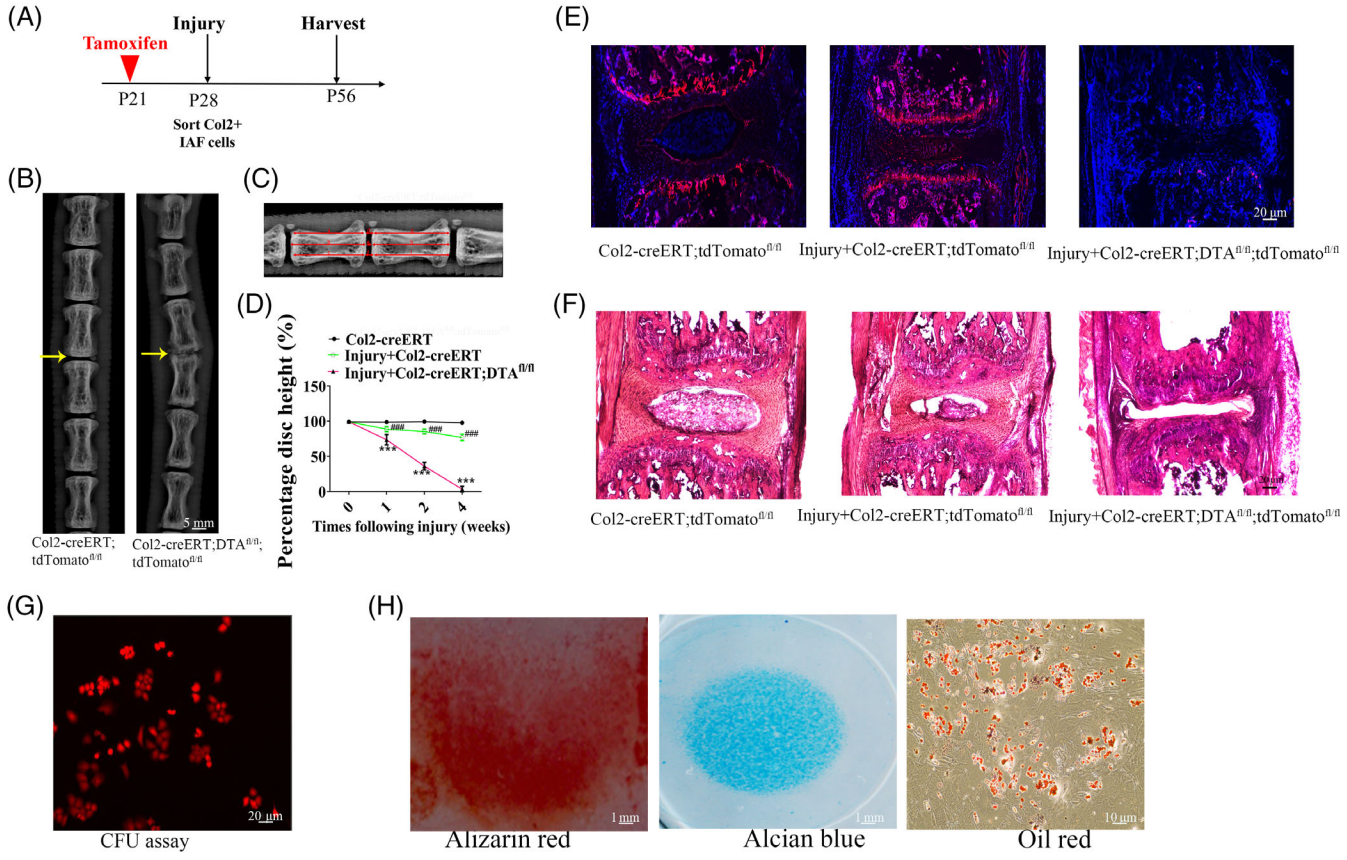

FIGURE 7 Col2+ progenitors are important for intervertebral disc (IVD) repair. A, The illustration of the experiment design. B, Representative of X-ray images in Col2-creERT;tdTomato and Col2-creERT;DTA$^{fl/fl}$ mice. Yellow arrow: the injured IVD in each group. Scale bar = 5 mm. C, Measurement protocol for the determination of the DHI calculated as [(d + e + f)/(a + b + c + g + h + i) ×100%]. D, DHI at different time-points following injury. Values are expressed as the mean ± SD (n = 10). DHI, disc height index (n = 6 mice per condition from three independent experiments). Data are mean ± SD. E, Representative fluorescent images of coronal sections of IVD in intact Col2-creERT;tdTomato, injured Col2-creERT;tdTomato, and Col2-creERT;DTA$^{fl/fl}$;tdTomato mice. Scale bar = 20 μm. F, Representative H&E images of coronal sections of IVD in intact Col2-creERT, injured Col2-creERT and Col2-creERT;DTA$^{fl/fl}$ mice. Scale bar = 20 μm. G, CFU-F assay in Col2+ IAF progenitor. Scale bar = 20 μm. H, Trilineage differentiation of Col2+ progenitors. Osteogenic (left), chondrogenic (center), and adipogenic (right) differentiation conditions. Statistical significance was determined by one-way ANOVA and Student's *t* test. **P* < .05, ***P* < .01, ****P* < .0001. NS, not statistically significant. Scale bar = 10 μm

chondrogenic, and adipogenic media, respectively. Figure 7H shows that Col2+ cells have differentiation potential to tri-lineages including chondrocytes (Alcian blue+ spheres), osteoblasts (Alizarin red+ mineralized matrix), and adipocytes (Oil Red+). All these findings suggested Col2+ cells are the important progenitors for IVD repair.

4 | DISCUSSION

In this study, we revealed for the first time that embryonic Col2+ cells ablation led to completely loss of spine. To our knowledge, it is also the first time to report the mouse model with complete loss of spine formation but reservation of surrounding soft tissues including spine cord. In agreement with cell ablation results, genetic lineage tracing of Col2-cre;tdTomato mice revealed that the majority of cells in spine are Col2+ but the surrounding muscle are Col2−. In vertebrates, somites develop into the main components of the paraxial skeleton, including the spine.[1,32] The dorsal portion of the somite differentiates into muscle and dermis, whereas the ventral counterpart gives rise to the skeletal elements of the spine.[1] According to our lineage tracing and cell ablation results, the embryonic Col2+ cells may contribute to ventral counterpart of the somite development.

Our results further showed that postnatal ablation of Col2+ cells caused severe delay and defects in spine development. The lineage tracing results from 4-week-old Col2-creERT;tdTomato mice showed tdTomato+ signaling is present in the IAF, EP, GP, and some bone cells in vertebral bone, but not in the NP when Cre was induced at P3. Consistently, histological results suggested the pattern of IVD, and vertebral bones were dramatically disrupted: GP and EP are shortened with less and disorganized Col2+ cells in GP, EP, and IAF. Interestingly, although few cells are tdTomato+ in NP with postnatal lineage tracing, the dramatically disorganized NP cell alignment was detected in Col2+ cells ablated mice suggested the NP cells are indirectly affected by Col2+ cell ablation. So far, the source of collagen matrix surrounding NP is still unclear.[33] The fact that few cells were tdTomato+ cells in NP when Cre was induced at P3, suggesting that NP cannot secrete Col2α1. Additionally, our results showed that Col2α1 matrix is present surrounding NP in Col2-creERT;tdTomato mice which completely lost in Col2+ cell ablated mice, suggesting that the collagen matrix surrounding NP may be secreted by IAF or EP cells given the large numbers of cells in IAF and EP are Col2+. Therefore, the dramatically disorganized NP cells in Col2+ ablated mice may be succeeded to the reduction of ECM and changed surrounding environments, which need to be further investigated in the future.

It was reported that the number of Col2+ cell columns in the GP and articular cartilage of knee decreases after the TM pulse in age dependent manner.[34] By comparing the patterns of targeted cells, we found the percentage of the Col2+ progenitors and their differentiation ability in IVD are also decreased with age in vivo. The decreased Col2+ cells in each compartment of IVD are varied depending on the age. Col2+ progenitors decreased most from embryonic to P0 in NP, from newborn to P21 in EP, from P21 to P30 in IAF, and from 6 months to 1-year-old in GP. The dynamic and sequential reduction of Col2+ cells in each compartment of IVD tissues with age suggested Col2+ cells may dominantly contribute to individual IVD compartment developmental and function at different stages.[35]

Previous studies[36] indicated that nuclear Cre activity from the Col2-creERT allele is limited to cells expressing Col2α1 at approximately 24 to 72 hours after TM administration. Consistently with these results, we found that Col2α1 is expressed in IAF and EP in IVD at P6 after TM injection at P3. Interestingly, Col2α1 expression were found to be enriched in the gel-like matrix surrounding the NP at P30 and P187, whereas Col2α1expressed cells in Col2-creERT;tdTomato mice are dramatically decreased when TM was injected at P27 and P184 comparing with P5. This difference is likely because nuclear Cre activity from the Col2-creERT allele is limited to the cells expressing Col2α1 with TM administration, while the Col2+ ECM expression detected by immunostaining with Col2α1 antibody reflected the balance among Col2α1 secretion, degradation, and accumulation.[19,37,38] Most interestingly, our results showed that Col2α1+ signaling locates in the gel-like matrix surrounding the NP cells at early stage of P3 to P187 and then dominantly locates in NP cells at P365. These results suggest that notochordal cells undergo terminal differentiation to give rise to chondrocyte-like cells[13,17] that can happen between 6 month and 1-year-old in mouse.[39]

It was reported that progenitor cells can be detected in various compartments of the IVD.[40] In injury-induced IVDD, neonates underwent IVD healing with functional restoration and enhanced structural repair after herniation.[41] However, the cell resource and cell type that contributes to IVD repair are still unclear. In agreement with previous studies,[41] we found that IVD can heal when the mice were injured at 3-week-old mice. Very interesting, we observed that a large population of Col2+ cells can be detected at injured site at 4 weeks follow the injury. By ablating Col2+ cell in mice, we found that severe IVDD and few Col2+ cells existing in injured site. Moreover, our in vitro study showed that the Col2+ cells from injured site possess tri-lineage differentiation potential and clonogenicity suggested Col2+ represented progenitor cells. Thus, these results revealed that Col2+ progenitors are essential for injury-induced IVD repair. With the development of tissues and engineering, cell-based therapy was regarded as a promising and effective approach for treating IVDD.[42,43] Previously, the choice of cell type is mainly focused on stem cells and NP cells. Recently, Chen et al[44] reported that the injection of fibroblasts into degenerated IVD could maintain the IVD height in cynomolgus monkeys. Considering the strong regenerative ability of Col2+ cells, the delivery of Col2+ cells could be a promising approach for treating IVDD in the future.

5 | CONCLUSION

In summary, our study for the first time, reveal that Col2+ cells are major progenitor cells for spine and IVD development and maintenance. Col2+ progenitors are essential contributors to the injury-induced IVD repair. Thus, our findings provide new insights into the spine or IVD development and promising therapeutic strategies for IVDD repair and regeneration.

ACKNOWLEDGMENTS

Research reported in this publication was supported by the National Institute of Dental and Craniofacial Research and the National Institute of Arthritis and Musculoskeletal and Skin Diseases, and National Institute on Aging, part of the National Institutes of Health, under Award Numbers DE023105, AR066101, and AG048388 to S. Yang. X. Li was supported by China Scholarship Council (CSC) Grant 201706260178. The content is solely the responsibility of the authors and does not necessarily represent the official views of the National Institutes of Health.

CONFLICT OF INTEREST

The authors declared no potential conflicts of interest.

AUTHOR CONTRIBUTIONS

X.L.: performed the experiments, interpreted the data and wrote the initial draft of the manuscript; S.T.Y.: managed mice colonies and assisted with the experiments; L.Q.: provided critical suggestions, reagents and technical assistance during the study; S.Y.: performed the experiments, interpreted the data and wrote the initial draft of the manuscript, conceived, supervised the study and wrote the manuscript.

DATA AVAILABILITY STATEMENT

The data that support the findings of this study are available on request from the corresponding author.

ORCID

Ling Qin https://orcid.org/0000-0002-2582-0078
Shuying Yang https://orcid.org/0000-0002-7126-6901

REFERENCES

1. Kaplan KM, Spivak JM, Bendo JA. Embryology of the spine and associated congenital abnormalities. *Spine J*. 2005;5(5):564-576.
2. Grimme JD, Castillo M. Congenital anomalies of the spine. *Neuroimaging Clin N Am*. 2007;17(1):1-16.
3. Chen S, Feng J, Zhang H, Jia M, Shen Y, Zong Z. Key role for the transcriptional factor, osterix, in spine development. *Spine J*. 2014;14(4):683-694.
4. Fleming A, Kishida MG, Kimmel CB, Keynes RJ. Building the backbone: the development and evolution of vertebral patterning. *Development*. 2015;142(10):1733-1744.
5. Scaal M. Early development of the vertebral column. *Semin Cell Dev Biol*. 2016;49:83-91.
6. Kester L, van Oudenaarden A. Single-cell transcriptomics meets lineage tracing. *Cell Stem Cell*. 2018;23(2):166-179.
7. Ono N, Balani DH, Kronenberg HM. Stem and progenitor cells in skeletal development. *Curr Top Dev Biol*. 2019;133:1-24.
8. Yue R, Zhou BO, Shimada IS, Zhao Z, Morrison SJ. Leptin receptor promotes adipogenesis and reduces osteogenesis by regulating mesenchymal stromal cells in adult bone marrow. *Cell Stem Cell*. 2016;18(6):782-796.
9. Zhou BO, Yue R, Murphy MM, Peyer JG, Morrison SJ. Leptin-receptor-expressing mesenchymal stromal cells represent the main source of bone formed by adult bone marrow. *Cell Stem Cell*. 2014;15(2):154-168.
10. Abzhanov A, Rodda SJ, McMahon AP, et al. Regulation of skeletogenic differentiation in cranial dermal bone. *Development*. 2007;134(17):3133-3144.
11. Debnath S, Yallowitz AR, McCormick J, et al. Discovery of a periosteal stem cell mediating intramembranous bone formation. *Nature*. 2018;562(7725):133-139.
12. Mizuhashi K, Ono W, Matsushita Y, et al. Resting zone of the growth plate houses a unique class of skeletal stem cells. *Nature*. 2018;563(7730):254-258.
13. McCann MR, Tamplin OJ, Rossant J, et al. Tracing notochord-derived cells using a Noto-cre mouse: implications for intervertebral disc development. *Dis Model Mech*. 2012;5(1):73-82.
14. Ono N, Ono W, Nagasawa T, Kronenberg HM. A subset of chondrogenic cells provides early mesenchymal progenitors in growing bones. *Nat Cell Biol*. 2014;16(12):1157-1167.
15. Serowoky MA, Arata CE, Crump JG, Mariani FV. Skeletal stem cells: insights into maintaining and regenerating the skeleton. *Development*. 2020;147(5):dev179325.
16. Matsushita Y, Ono W, Ono N. Skeletal stem cells for bone development and repair: diversity matters. *Curr Osteoporos Rep*. 2020;18:189-198.
17. Tong W, Lu Z, Qin L, et al. Cell therapy for the degenerating intervertebral disc. *Transl Res*. 2017;181:49-58.
18. Wei Y, Tower RJ, Tian Z, et al. Spatial distribution of type II collagen gene expression in the mouse intervertebral disc. *JOR Spine*. 2019;2(4):e1070.
19. Ovchinnikov DA, Deng JM, Ogunrinu G, Behringer RR. Col2a1-directed expression of Cre recombinase in differentiating chondrocytes in transgenic mice. *Genesis*. 2000;26(2):145-146.
20. Nakamura E, Nguyen MT, Mackem S. Kinetics of tamoxifen-regulated Cre activity in mice using a cartilage-specific CreER(T) to assay temporal activity windows along the proximodistal limb skeleton. *Dev Dyn*. 2006;235(9):2603-2612.
21. Madisen L, Zwingman TA, Sunkin SM, et al. A robust and high-throughput Cre reporting and characterization system for the whole mouse brain. *Nat Neurosci*. 2010;13(1):133-140.
22. Voehringer D, Liang HE, Locksley RM. Homeostasis and effector function of lymphopenia-induced "memory-like" T cells in constitutively T cell-depleted mice. *J Immunol*. 2008;180(7):4742-4753.
23. Henry SP, Jang CW, Deng JM, Zhang Z, Behringer RR, de Crombrugghe B. Generation of aggrecan-CreERT2 knockin mice for inducible Cre activity in adult cartilage. *Genesis*. 2009;47(12):805-814.
24. Yuan X, Yang S. Deletion of IFT80 impairs epiphyseal and articular cartilage formation due to disruption of chondrocyte differentiation. *PLoS One*. 2015;10(6):e0130618.
25. Yoon SJ, Kim EC, Noh K, Lee DW. Supramolecular hydrogels based on MPEG-grafted hyaluronic acid and alpha-CD containing HP-beta-CD/simvastatin enhance osteogenesis in vivo. *J Nanosci Nanotechnol*. 2017;17(1):217-223.
26. Li X, Yang S, Han L, Mao K, Yang S. Ciliary IFT80 is essential for intervertebral disc development and maintenance. *FASEB J*. 2020;34(5):6741-6756.
27. Li X, Liu X, Wang Y, et al. Intervertebral disc degeneration in mice with type II diabetes induced by leptin receptor deficiency. *BMC Musculoskelet Disord*. 2020;21(1):77.
28. Li Q, Qu F, Han B, et al. Micromechanical anisotropy and heterogeneity of the meniscus extracellular matrix. *Acta Biomater*. 2017;54:356-366.
29. Nakamichi R, Ito Y, Inui M, et al. Mohawk promotes the maintenance and regeneration of the outer annulus fibrosus of intervertebral discs. *Nat Commun*. 2016;7:12503.
30. Zhong L, Yao L, Tower RJ, et al. Single cell transcriptomics identifies a unique adipose lineage cell population that regulates bone marrow environment. *Elife*. 2020;131(2):e140214.
31. Hatano E, Fujita T, Ueda Y, et al. Expression of ADAMTS-4 (aggrecanase-1) and possible involvement in regression of lumbar disc herniation. *Spine (Phila Pa 1976)*. 2006;31(13):1426-1432.

32. Ashley JW, Enomoto-Iwamoto M, Smith LJ, et al. Intervertebral disc development and disease-related genetic polymorphisms. *Genes Dis*. 2016;3(3):171-177.
33. Lyu FJ, Cheung KM, Zheng Z, Wang H, Sakai D, Leung VY. IVD progenitor cells: a new horizon for understanding disc homeostasis and repair. *Nat Rev Rheumatol*. 2019;15(2):102-112.
34. Nagao M, Cheong CW, Olsen BR. Col2-Cre and tamoxifen-inducible Col2-CreER target different cell populations in the knee joint. *Osteoarthr Cartil*. 2016;24(1):188-191.
35. Alkhatib B, Ban GI, Williams S, Serra R. IVD development: nucleus pulposus development and sclerotome specification. *Curr Mol Biol Rep*. 2018;4(3):132-141.
36. Shi Y, He G, Lee WC, McKenzie JA, Silva MJ, Long F. Gli1 identifies osteogenic progenitors for bone formation and fracture repair. *Nat Commun*. 2017;8(1):2043.
37. Tryfonidou MA, Lunstrum GP, Hendriks K, et al. Novel type II collagen reporter mice: new tool for assessing collagen 2alpha1 expression in vivo and in vitro. *Dev Dyn*. 2011;240(3):663-673.
38. Sakai K, Hiripi L, Glumoff V, et al. Stage-and tissue-specific expression of a Col2a1-Cre fusion gene in transgenic mice. *Matrix Biol*. 2001;19 (8):761-767.
39. Risbud MV, Schoepflin ZR, Mwale F, et al. Defining the phenotype of young healthy nucleus pulposus cells: recommendations of the Spine Research Interest Group at the 2014 annual ORS meeting. *J Orthop Res*. 2015;33(3):283-293.
40. Liang L, Li X, Li D, et al. The characteristics of stem cells in human degenerative intervertebral disc. *Medicine (Baltimore)*. 2017;96(25): e7178.
41. Torre OM, Das R, Berenblum RE, Huang AH, Iatridis JC. Neonatal mouse intervertebral discs heal with restored function following herniation injury. *FASEB J*. 2018;32(9):4753-4762.
42. Chu G, Shi C, Lin J, et al. Biomechanics in annulus fibrosus degeneration and regeneration. *Adv Exp Med Biol*. 2018;1078: 409-420.
43. Gullbrand SE, Ashinsky BG, Bonnevie ED, et al. Long-term mechanical function and integration of an implanted tissue-engineered intervertebral disc. *Sci Transl Med*. 2018;10(468):eaau0670.
44. Chen C, Zhou T, Sun X, et al. Autologous fibroblasts induce fibrosis of the nucleus pulposus to maintain the stability of degenerative intervertebral discs. *Bone Res*. 2020;8:7.

SUPPORTING INFORMATION

Additional supporting information may be found online in the Supporting Information section at the end of this article.

How to cite this article: Li X, Yang S, Qin L, Yang S. Type II collagen-positive embryonic progenitors are the major contributors to spine and intervertebral disc development and repair. *STEM CELLS Transl Med*. 2021;10:1419–1432. https://doi.org/10.1002/sctm.20-0424